



## Supplementary Material for **Spatiotemporal light control with frequency-gradient metasurfaces**

Amr M. Shaltout, Konstantinos G. Lagoudakis, Jorik van de Groep, Soo Jin Kim,  
Jelena Vučković, Vladimir M. Shalaev, Mark L. Brongersma\*

\*Corresponding author. Email: [brongersma@stanford.edu](mailto:brongersma@stanford.edu)

Published 26 July 2019, *Science* **365**, 374 (2019)

DOI: [10.1126/science.aax2357](https://doi.org/10.1126/science.aax2357)

### **This PDF file includes:**

Materials and Methods  
Supplementary Text S1 to S3  
Figs. S1 to S4

### **Other Supplementary Material for this manuscript includes the following:**

(available at [science.sciencemag.org/content/365/6451/374/suppl/DC1](https://science.sciencemag.org/content/365/6451/374/suppl/DC1))

Movies S1 to S4

## MATERIALS AND METHODS

### *Device Fabrication and Measurements:*

The experimental setup for our measurements of the beam steering action of the virtual frequency-gradient metasurface is depicted in Fig 2A. The coherent light source used here is a picosecond pulsed Ti:Sapphire mode-locked laser with an 80MHz repetition rate, generating a train of  $\sim 2.5$ ps pulses. A synchroscan streak camera locked to the pulsed laser provides information in time with approximately 2 ps temporal resolution. By bringing the focal point of a microscope objective with NA = 0.4 at the virtual frequency-gradient plane located at  $f_c$  from the Si-based metasurface, we map all incoming angles  $\theta$  to the axial dimension  $y_1$  at the microscope objective back focal plane  $f_{M.O.} = 0.3$  cm (note that the metasurface was designed to have  $f_c = 1$  cm and  $\theta_i = 45^\circ$ ). In order to match the physical size of the objective back focal plane axial dimension  $y_1$  to the size of the input slits of the streak camera (Hamamatsu Synchroscan), we use a two-lens 4f imaging system to scale down the spatial extend ( $y_2 = -\frac{f_2}{f_1}y_1$  with  $f_1 = 30$  cm and  $f_2 = 10$  cm).

### *Passive Si Metasurface Fabrication:*

500 nm thick c-Si on sapphire substrates are obtained commercially from MTI-Corp and diced in 2 cm  $\times$  2 cm. After cleaning the substrates by ultra-sonication in acetone and isopropanol, the substrates are spin coated with  $83 \pm 3$  nm of hydrogen silsesquioxane (HSQ, XR-1054-004, 4% in MIBK), which is a high-resolution negative-tone electron-beam resist. After a 45 min pre-exposure bake at 90 °C, a conductive polymer (e-spacer) is spin coated on top to prevent charging effects in the non-conductive substrate during exposure. A macroscopic array (8 mm  $\times$  4 mm) of nano-rods with dimensions (180 nm  $\times$  110 nm) and 350 nm spacing is written in the HSQ resist using a JEOL JBL 6300 100 kV system. The exposure was optimized for speed by using a 9.3 nA beam current, at the expense of lower resolution and spatial inhomogeneities. The structures in Fig. 2B-C are representative for the best areas, while some areas show

small deviations in antenna dimensions. After exposure, the conductive polymer is removed by rinsing in water, followed by development of the HSQ by dipping the sample in tetramethylammonium hydroxide (TMAH, 25% in water) for 120 s. Next, the HSQ nanopattern is transferred into the 500 nm thick Si by reactive-ion etching using a mixture of  $\text{Cl}_2$  and HBr. Finally, the HSQ mask is removed using HF (5% in water).

## SUPPLEMENTARY SECTIONS

### S1. Analytical Formulation of Frequency-Gradient Beam Steering:

In this section, we present the full mathematical proof for the beam steering action that is achievable with a frequency-gradient metasurface. Let the temporal properties of the incident pulse comprised of  $2N+1$  frequency lines be described as:

$$a(t) = \sum_{n=-N}^{n=N} a_n e^{-i\omega_n t} = e^{-i\omega_0 t} \sum_{n=-N}^{n=N} a_n e^{-in\Delta\omega t} = A(t) e^{-i\omega_0 t}, \quad (\text{S.1})$$

where  $A(t)$  is the envelope of the pulse. After interaction with the designed passive metasurface (See Fig 1C of the main text), each spectral (line) component is transformed into a distinct spatial optical mode ( $a_n \rightarrow b_n(\mathbf{r})$ ). The metasurface is judiciously designed to provide an optical mode in the form:

$$b_n(\mathbf{r}) = a_n G(\mathbf{r} - \mathbf{r}_n) e^{ik_n(|\mathbf{r} - \mathbf{r}_n|)}, \quad (\text{S.2})$$

where  $\mathbf{r}_n = (0, nd)$ ,  $d$  is the spacing between two adjacent sources, and  $G(\mathbf{r} - \mathbf{r}_n)$  is a slowly varying envelope that governs the angular divergence of the radiation pattern and  $e^{ik_n(|\mathbf{r} - \mathbf{r}_n|)}$  is a fast varying phase term. The resulting spatiotemporal pattern in the far-field takes the following form:

$$b(\mathbf{r}, t) = \sum_{n=-N}^{n=N} b_n(\mathbf{r}) e^{-i\omega_n t} = \sum_{n=-N}^{n=N} a_n G(\mathbf{r} - \mathbf{r}_n) e^{i(k_n |\mathbf{r} - \mathbf{r}_n| - \omega_n t)}, \quad (\text{S.3})$$

where the spatial coordinate  $\mathbf{r} = (x, y) = (r \cos \theta, -r \sin \theta)$  is represented in terms of the distance  $r$  from the center of the array  $(0,0)$ , and the clockwise angle  $\theta$  as shown in Fig 1C. In the far-field ( $r \gg Nd$ ), the slowly varying envelope is approximately the same for all the summation terms ( $G(\mathbf{r} - \mathbf{r}_n) \approx G(\mathbf{r})$ ), and the distance  $|\mathbf{r} - \mathbf{r}_n|$  can be approximated as:

$$|\mathbf{r} - \mathbf{r}_n| = \sqrt{(r \sin \theta + nd)^2 + r^2 \cos^2 \theta} \approx r + nd \sin \theta.$$

This leads to:

$$b(\mathbf{r}, t) \approx G(\mathbf{r}) e^{i(k_o r - \omega_o t)} \sum_{n=-N}^{n=N} a_n e^{in(\Delta k r + k_o d \sin \theta - \Delta \omega t)}. \quad (\text{S.4})$$

By comparing equations (S.1) and (S.4) we can find that:

$$b(\mathbf{r}, t) \approx A \left( t - \frac{k_o d}{\Delta \omega} \sin \theta - \frac{r}{c} \right) G(\mathbf{r}) e^{i(k_o r - \omega_o t)}, \quad (\text{S.5})$$

which is Eq (2) in the main manuscript that captures the beam steering action. The term  $r/c$  simply accounts for the propagation delay between the frequency-gradient metasurface and the point of detection at a distance  $r$ . For a cylindrical surface at a fixed distance  $r$ , the time-dependent steering angle can be written as:

$$\sin \theta = \left( \frac{\Delta \omega}{k_o d} \right) t, \quad (\text{S.6})$$

after translating the time reference  $t \equiv t - \frac{r}{c}$ . Eq (S.5) determines the angular steering speed of light to be proportional to the frequency-gradient ratio  $(\Delta \omega / d)$ . Figure S1 demonstrates the impact of the frequency-gradient metasurface on the input temporal pulse  $|a(t)|^2$  producing a spatiotemporal pattern  $|b(\mathbf{r}, t)|^2$ .

It's worth noting that the angular steering speed, and the repetition rate can independently controlled. According to Eq(S.5), the temporal repetition rate of the spatiotemporal beam  $b(\mathbf{r}, t)$  is the same repetition rate of the envelope function  $A(t)$  which is solely dependent on the spectral spacing between frequency-comb lines  $\Delta\omega$ , with a repetition period  $\tau = 2\pi/\Delta\omega$ . Then controlling the spacing  $d$  allows one to independently change the steering speed for the same repetition rate. This means that it's possible for the scanning time to be smaller or bigger then the repetition period  $\tau$ . In order to adjust the scanning time for a full angle of view (i.e.  $\sin \theta$  changes from -1 to 1) to be the same as the repetition rate  $\tau$ , in accordance with to Eq (S.6), we obtain:

$$2 = \left(\frac{\Delta\omega}{k_0 d}\right) \tau \Rightarrow d = \frac{\lambda_0}{2}. \quad (\text{S.7})$$

In case  $d < \frac{\lambda_0}{2}$ , the steering time is smaller than  $\tau$ , which means that there will be some time without a laser beam till the following repetition period. On the other hand, if  $d > \frac{\lambda_0}{2}$ , one can have a situation where more than one beam in different directions can be present at the same instant.

## **S2. Simulations of Frequency-Gradient Beam Steering:**

Figure S2 shows numerical simulations of the intensity  $I(\mathbf{r}, t) = |b(\mathbf{r}, t)|^2$  where  $b(\mathbf{r}, t)$  is calculated according to Eq. (4) in the main manuscript, with  $\lambda_0 = 720 \text{ nm}$  and  $d = 360 \text{ nm}$ , for  $\Delta\omega = 2\pi \times 10 \text{ GHz}$  and  $\Delta\omega = 2\pi \times 100 \text{ GHz}$ . As time evolves, the laser beam scans clockwise. The scanning time is reduced by 10 times as the frequency gradient ( $\Delta\omega/d$ ) is multiplied by 10. Video simulations of these two cases are presented in Movie S1 and Movie S2.

The previous simulations are adjusted for  $d = \frac{\lambda_0}{2}$  according to Eq. (S.7) in order to adjust the repetition period to match the scanning time. This is why in the steering beams in Movie S1 and Movie S2 start a new scanning period at the instant the previous scan ends. Movie S3 shows the

case where  $d < \frac{\lambda_o}{2}$  ( $d = \frac{\lambda_o}{4} = 180 \text{ nm}$ ), in which scanning occurs only over half of the repetition period. On the other hand, Movie S4, shows the case where  $d > \frac{\lambda_o}{2}$  ( $d = \lambda_o = 720 \text{ nm}$ ), in which two different beams exist at the same instant.

### S3. Effect of the Si Metasurface on Spectral Components:

Figure S3(A) demonstrates the standard technique to resolve the spectral components of an ultrafast optical source onto an array of focal lines at a specific focal plane. It typically consists of a diffraction grating cascaded by a cylindrical lens. Light incident onto the diffraction grating will split into a slightly different direction for each spectral component, which in turn will get focused into different lines along the focal plane of the lens due to the changing angle of incidence on the lens. The array of focused spectral components acts as our sought-after frequency-gradient source.

Figure S3(B) helps us to evaluate the frequency gradient ( $\Delta\omega/d$ ) at the focal plane. Suppose the incident angle is defined so that the central frequency component having a frequency  $\omega_o$  ( $\lambda_o = 720 \text{ nm}$ ) and a wavenumber  $k_o$  be transmitted parallel to the lens axis in order to be focused onto the axis. In this case, any other frequency component  $\omega_o + \Delta\omega$  (wavenumber  $k_o + \Delta k$ ) will be transmitted from the grating at a slightly different direction from the normal, as shown in Fig S3(B). This means it will have some tangential wavenumber component  $k_t$ , which implies that the spectral component  $\omega_o + \Delta\omega$  will have an off-axis focusing spot at a distance  $d$  from the axis. For the assumed condition  $k_t \ll k_o$ , we can use the paraxial approximation:

$$\frac{d}{f_c} = \frac{k_t}{k_o}, \quad (\text{S.8})$$

where  $f_c$  is the focal distance of the lens. We can replace each of the diffraction grating and lens using phase gradient metasurfaces (a meta-grating and a meta-lens) as shown in Fig. S3(B). The

phase profile of the meta-grating is of the form ( $\phi_{m1} = -k_o \sin\theta_i x$ ) where  $x$  is the spatial dimension along the metasurface, such that the tangential wavenumber component at the center frequency component  $\omega_o$  is cancelled out, and any other spectral components with frequency of the form  $\omega_o + \Delta\omega$  have a tangential wavenumber component of  $k_t = \Delta k \sin\theta_i = \frac{\Delta\omega}{c} \sin\theta_i$ . When light goes through the meta-lens of focal distance  $f_c$  with phase-gradient ( $\phi_{m2} = -k_o (f_c - \sqrt{f_c^2 + x^2})$ ), then it is focused at an off-axis distance  $d$  proportional to the frequency shift  $\Delta\omega$  according to eq (S.6). Therefore, a virtual frequency-gradient metasurface is created at the focal plane where the frequency gradient  $\Delta\omega/d$  is calculated as:

$$\frac{\Delta\omega}{d} = \frac{\omega_o}{f_c \sin\theta_i}. \quad (\text{S.9})$$

Furthermore, the system can be reduced to a single metasurface by combining the phase profiles of both the meta-grating and the meta-lens into a single metasurface with the phase profile ( $\phi_m = \phi_{m1} + \phi_{m2}$ ) as shown in Fig S3(D), which will focus the spectral components of the input source into different spots on the focal plane using a single step. Therefore, a virtual frequency-gradient metasurface is created at the focal plane using a pulsed source with frequency-comb spectrum and a single phase-gradient metasurface. Light diffracts again from the frequency-gradient into the far-field zone to interfere spatiotemporally according to Eq. (S.5) to perform the beam steering action.

The metasurface is implemented using crystalline silicon on top of sapphire substrate, and the design dimensions of the single nano-antennas are 110 nm x 180 nm, with a height of 500 nm, and a periodicity of 350 nm in both transverse directions. The metasurface induces a geometric phase-shift for circularly polarized light controlled by the orientation of the nano-antennas. The transmission diffraction efficiency of the gemetric phase gradient metasurfaces is given by:

$$T = \frac{n}{4} |t_{\perp} - t_{\parallel}|^2 \quad (\text{S.10})$$

where  $t_{\perp}$  and  $t_{\parallel}$  are the transmission coefficients along the major and minor axis of the metasurface, and  $n$  is the refractive index of substrate. Figure S4 presents numerical simulations of the transmission diffraction efficiency of our Si nano-antenna structure as a function of wavelength. It should theoretically achieve an efficiency  $\sim 80\%$  within the operational bandwidth. However, there have been practical limitations because the large size of the metasurface (8 mm x 4 mm) favored the fabrication to be optimized for speed on the expense of resolution and spatial homogeneity. Therefore, our fabricated dimensions didn't match with the design, and also the large variations of these dimensions along the metasurface added an extra decoherence factor lowering the experimental efficiency, which has been measured to be 6.6% at the 720 nm central wavelength. However, dielectric metasurfaces can be transparent in principle, and large transmission efficiencies ( $>80\%$ ) have been achieved before (see ref 14 in main text).

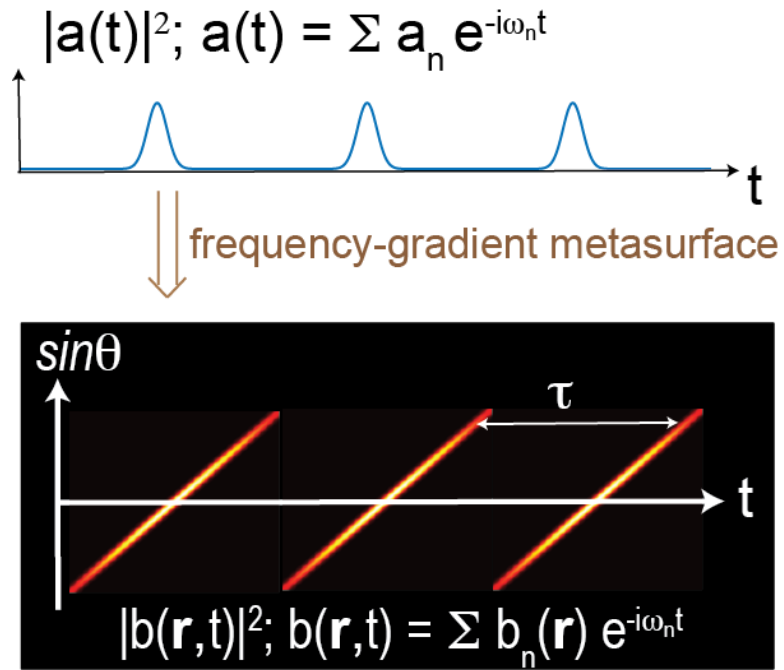


Figure S1.: Impact of the frequency-gradient metasurface transforming a temporal pulse into a spatiotemporal pulse as in Eq (S.5) where the beam intensity is a function of both angle and time.

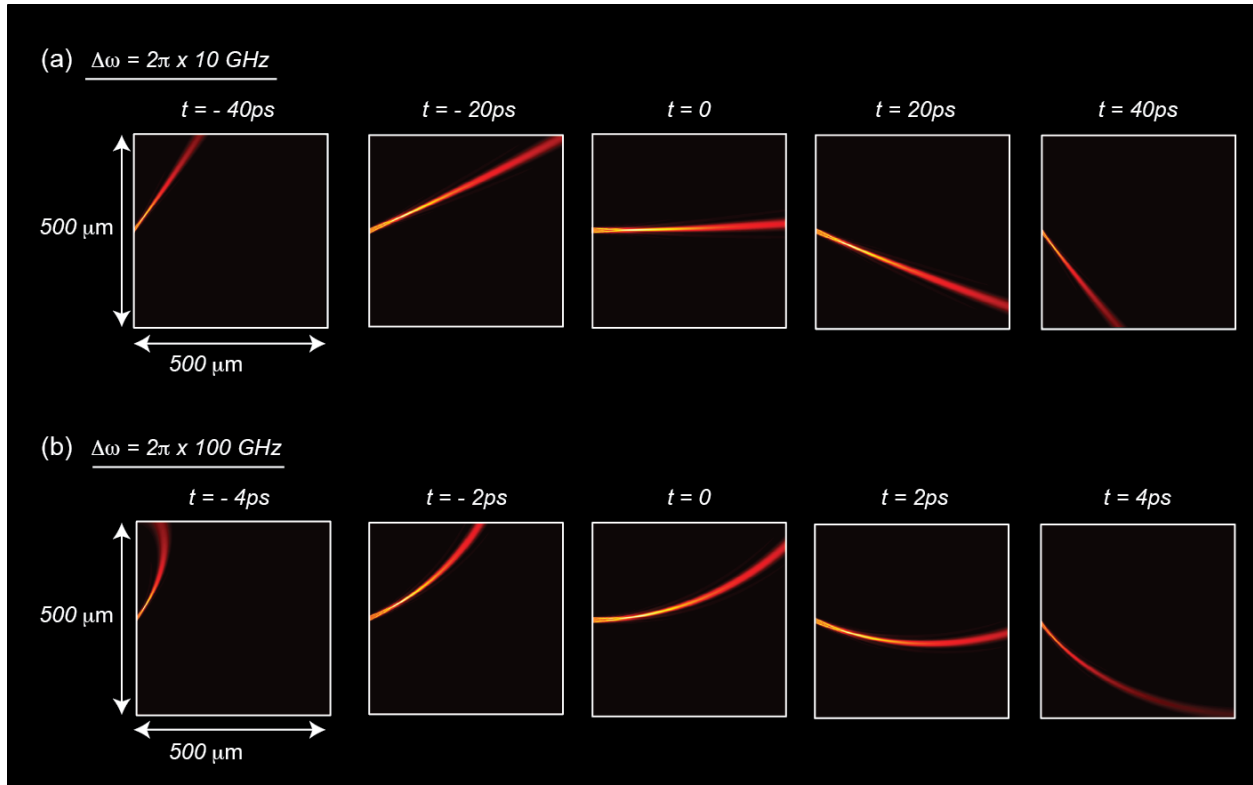


Figure S2: Optical radiation generated by a virtual frequency-gradient metasurface at different time instants and for different spectral spacing between the frequency lines of the illuminating frequency comb source. As time proceeds from left to right the optical beam scans clockwise. Video simulations of these two cases are provided in supplementary-video1 and supplementary-video2. A faster scanning rate is achieved for a larger frequency-gradient when  $\Delta\omega$  is increased. When the angular scanning time is comparable to the propagation time, the light beam displays a bending effect (similar to the apparent bending of the water beam emerging from a rotating water hose).

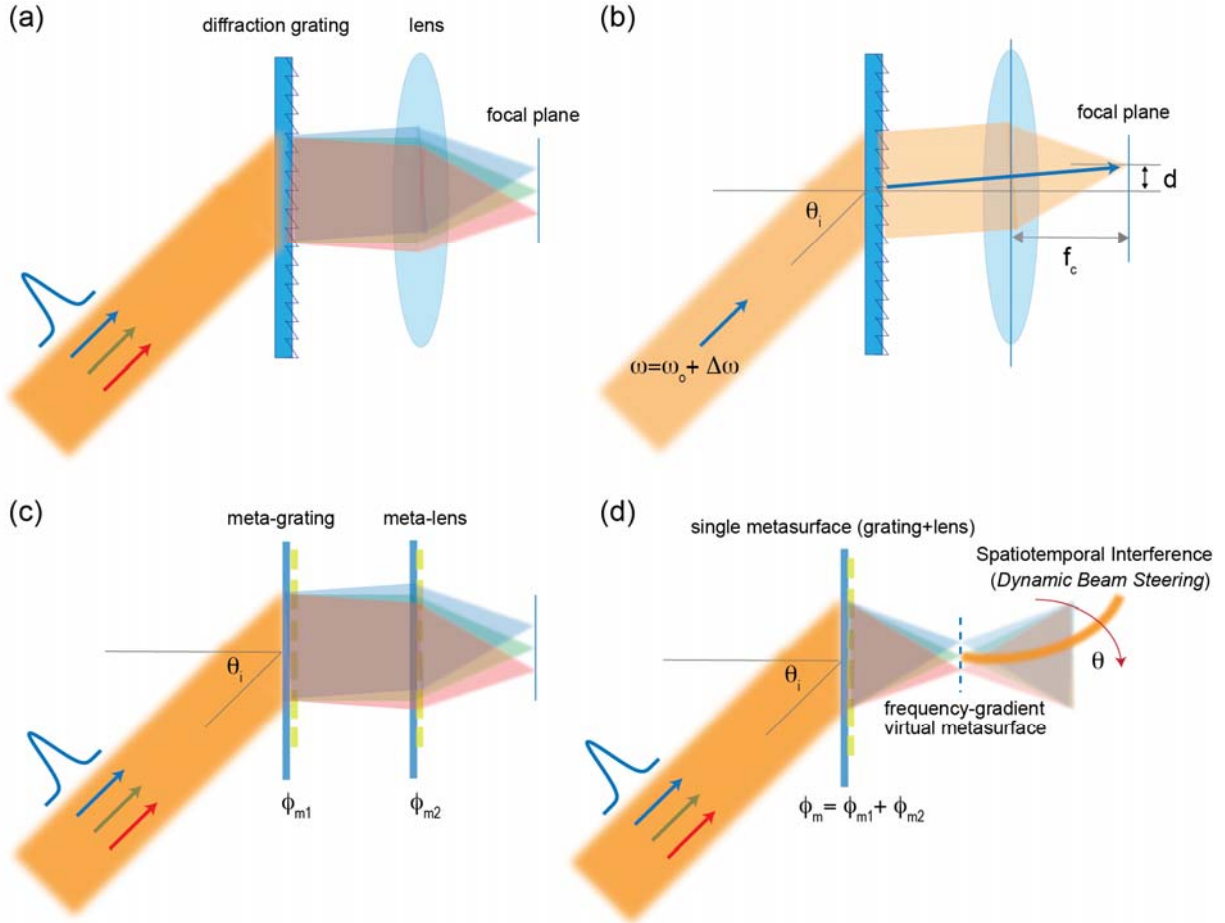


Fig S3: (A) Standard setup consisting of diffraction grating and cylindrical lens utilized to resolve the spectral components of a pulsed source into different focusing lines at a specific focal plane. (B) Demonstration of the effect of tuning the frequency of the incident light by  $\Delta\omega$  on shifting the focal spot by a distance  $d$  across the focal plane. (C) Replacement of diffraction grating and convex lens by a meta-grating and meta-lens implemented using phase-gradient metasurfaces with phase profiles ( $\phi_{m1} = -k_o \sin\theta_i x$ ) and ( $\phi_{m2} = -k_o (f_c - \sqrt{f_c^2 + x^2})$ ). (D) Combining the meta-grating and meta-lens into a single phase gradient metasurface with the phase profile ( $\phi_m = \phi_{m1} + \phi_{m2}$ ).

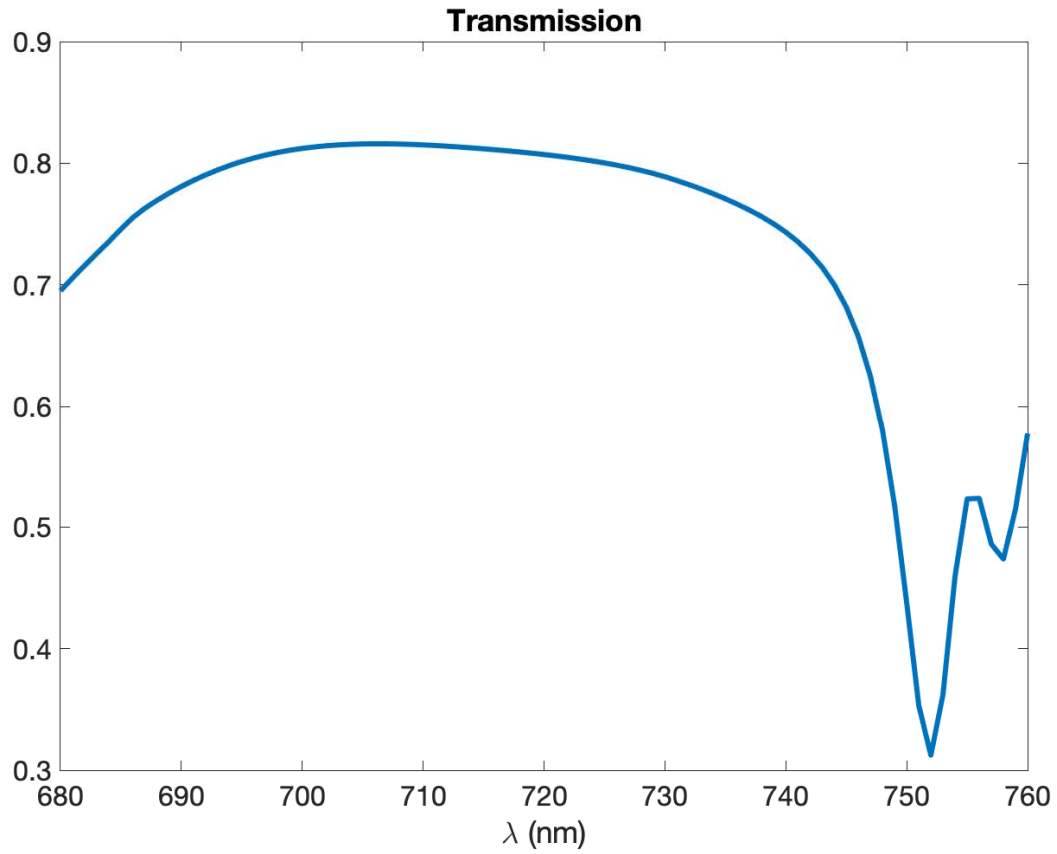


Fig. S4: Finite-element-method (FEM) of the transmission diffraction efficiency of the Si based nano-antenna structure as a function of wavelength.